Dual-Modal Nanoprobes for Imaging of Mesenchymal Stem Cell Transplant by MRI and Fluorescence Imaging

Chang Kyu Sung, MD[1]
Kyung Ah Hong, MD[1]
Shunmei Lin, MD[1]
Yuwon Lee, MD[2]
Jinmyung Cha, MD[2]
Jin-Kyu Lee, MD[2]
Cheol Pyo Hong, MD[3]
Bong Soo Han, MD[3]
Sung Il Jung, MD[4]
Seung Hyup Kim, MD[5]
Kang Sup Yoon, MD[6]

Index terms:
Stem cells
Nanoparticles
Magnetic resonance (MR)
Optical imaging, contrast agent

DOI:10.3348/kjr.2009.10.6.613

Korean J Radiol 2009;10:613-622
Received April 13, 2009; accepted after revision June 26, 2009.

[1]Department of Radiology, Seoul Metropolitan Boramae Medical Center, Seoul National University College of Medicine, Seoul 156-707, Korea; [2]Department of Chemistry, Seoul National University, Seoul 151-747, Korea; [3]Department of Radiological Science, College of Health Science, Yonsei University, Kangwon-do 220-710, Korea; [4]Department of Radiology, Konkuk University Medical Center, Konkuk University School of Medicine, Seoul 143-729, Korea; [5]Department of Radiology and the Institute of Radiation Medicine, Seoul National University College of Medicine, Seoul 110-744, Korea; [6]Department of Orthopedic Surgery, Seoul Metropolitan Boramae Medical Center, Seoul National University College of Medicine, Seoul 156-707, Korea

Address reprint requests to:
Chang Kyu Sung, MD, Department of Radiology, Seoul Metropolitan Boramae Medical Center, Seoul National University College of Medicine, 425 Shindaebang2-dong, Dongjak-gu, Seoul 156-707, Korea.
Tel. (822) 870-2533
Fax. (822) 870-2575
e-mail: sckmd@hanmail.net

Objective: To determine the feasibility of labeling human mesenchymal stem cells (hMSCs) with bifunctional nanoparticles and assessing their potential as imaging probes in the monitoring of hMSC transplantation.

Materials and Methods: The T1 and T2 relaxivities of the nanoparticles (MNP@SiO_2[RITC]-PEG) were measured at 1.5T and 3T magnetic resonance scanner. Using hMSCs and the nanoparticles, labeling efficiency, toxicity, and proliferation were assessed. Confocal laser scanning microscopy and transmission electron microscopy were used to specify the intracellular localization of the endocytosed iron nanoparticles. We also observed *in vitro* and *in vivo* visualization of the labeled hMSCs with a 3T MR scanner and optical imaging.

Results: MNP@SiO_2(RITC)-PEG showed both superparamagnetic and fluorescent properties. The r_1 and r_2 relaxivity values of the MNP@SiO_2(RITC)-PEG were 0.33 and 398 mM^{-1} s^{-1} at 1.5T, respectively, and 0.29 and 453 mM^{-1} s^{-1} at 3T, respectively. The effective internalization of MNP@SiO_2(RITC)-PEG into hMSCs was observed by confocal laser scanning fluorescence microscopy. The transmission electron microscopy images showed that MNP@SiO_2(RITC)-PEG was internalized into the cells and mainly resided in the cytoplasm. The viability and proliferation of MNP@SiO_2(RITC)-PEG-labeled hMSCs were not significantly different from the control cells. MNP@SiO_2(RITC)-PEG-labeled hMSCs were observed *in vitro* and *in vivo* with optical and MR imaging.

Conclusion: MNP@SiO_2(RITC)-PEG can be a useful contrast agent for stem cell imaging, which is suitable for a bimodal detection by MRI and optical imaging.

Recent studies suggest that mesenchymal stem cells (MSCs) show significant potential as a novel cellular therapy for tissue regeneration (1). The development of new stem cell-based therapies requires a quantitative and qualitative assessment of stem cell distribution to the target organs, differentiation outcome, and engraftment (2, 3). In particular, the monitoring of cell trafficking *in vivo* and distinguishing whether cellular regeneration originated from an exogenous cell source is a key issue for developing successful stem cell therapies (4, 5). Although magnetic resonance imaging (MRI), radionuclide imaging, and optical imaging are all used to track the transplanted cells, MRI is progressing towards playing an important role in the development of stem cell therapy because its ability to demonstrate anatomic details with high contrast and exquisite spatial resolution, and can noninvasively follow stem cells for long periods of time (6, 7).

The detection of the transplanted cells by MRI requires cells to be labeled magnetically either by endocytic internalizing or cell surface attachment of magnetic nanoparticles (MNPs) (8–11). Recently, a variety of magnetic nanoparticles such as superpara-

magnetic iron oxide (SPIO) have been developed. Although native iron oxide particles are used as the currently preferred cell-labeling materials, they have low intracellular labeling efficiency and the exposed metal ion on the surface of nanoparticles can cause metal elemental toxicities in cells (12–14). The surface coating of magnetic nanoparticles with polystyrene, dextran, and dendrimers have been reported to improve the cellular-internalization of contrast agent, but the efficiency of internalization is still generally low and it requires long-term incubation time and high concentration of particles (13–15). It is therefore highly desirable to develop a nanoparticle that is nontoxic, biocompatible, efficient at intracellular labeling, and highly sensitive to detection. The current challenges also include the development of multimodality imaging for compensating the limited MRI sensitivity and extending its application by combining the strengths of different imaging modalities.

Bifunctional contrast agents with both optical and magnetic contrast were made using various methods and demonstrated to serve as good molecular imaging probes for multimodality imaging (16–18). By incorporating organic fluorescent dye molecules into the silica-coated magnetite core-shell, we synthesized uniform dual-functionalized nanoparticles which permit dual-modality detections (19, 20). Recently, several noninvasive, MR-based monitoring methods were used to tract MSCs transplant. However, the bifunctional magnetofluorescent nanoparticles as a single molecule have rarely been applied in MSCs tracking prior to this study. We investigated the feasibility of labeling human mesenchymal stem cells (hMSCs) with bifunctional nanoparticles and assessed their potential as imaging probes in the monitoring of hMSC transplantation.

MATERIALS AND METHODS

Preparation of Magnetic Nanoparticles

The bifunctional nanoparticles were synthesized using a previously reported method (19, 20). Cobalt ferrite magnetic nanoparticles (MNP, $CoFe_2O_4$) were coated with a silica shell (SiO_2) of stable and biocompatible material to avoid the potential toxic effects on cells. To acquire additional fluorescent properties, an organic fluorescent dye (rhodamine B isothiocyanate, RITC) was incorporated into the silica shell. Thus, the MNP@SiO_2(RITC)s have a bifunctional property which enables dual modality detection by MRI and optical imaging. The surface of the dual-functionalized silica-coated nanoparticles was modified with biocompatible polyethylene glycol (PEG) groups to render them biocompatible by preventing the nonspecific adsorption of proteins to the nanoparticles. Attachment of the PEG did not significantly change the size of the nanoparticles. The average diameter of MNP@SiO_2(RITC)-PEG used in this study was about 50 nm. The characteristic properties of this compound are summarized in Table 1. The absorption (λmax) and emission maxima (λem) were observed at 540 and 625 nm, respectively.

Cell Culture

Human mesenchymal stem cells purchased from Cambrex (Cambrex, Walkersville, MD) were used for cell labeling. The cells were cultured in 75-cm^2 plastic culture flasks (BD, USA) in 8 ml of medium at 37° C, in a humidified incubator at 5% CO_2. The culture medium used was mesenchymal stem cell basal medium (MSCBM, Cambrex, Walkersville), which contains mesenchymal cell growth supplement (MCGS, Cambrex, Walkersville), 4 mM L-glutamine, and 100U Penicillin-Streptomycin. Next, the hMSCs were cultured under generally established cell conditions, transferred every three days, and split at a ratio of 1:5 upon confluence.

Determination of Cellular MNP@SiO_2(RITC)-PEG Uptake by Confocal Laser Scanning Fluorescence Microscopy

For the confocal imaging experiments, hMSCs were seeded and cultured onto Lab-Tek Chambered Coverglass (Nalge Nunc, Naperville, IL) at a density of 3×10^4 cells/cm^2 for 24 hours prior to labeling and staining. Next, the cells were cultured at different concentrations of MNP@SiO_2(RITC)-PEG for 2, 4, 6 hours in a 37° C humidified incubator maintained at 5% CO_2. After labeling, the cover slips were washed twice with cell culture medium and twice with phosphate buffer solution (PBS). The fluorescence images were obtained using a LSM 510 confocal microscope (Zeiss, Jena, Germany) equipped with Argon (458, 488, 514 nm) and HeNe (543, 633 nm) lasers for fluorescence. The exposure time for fluorescence was

Table 1. Characteristic Properties of MNP@SiO_2(RITC)-PEG

	MNP@SiO_2(RITC)-PEG
Cover structure	Polymer carboxydextran
Core	Cobalt ferrite nanoparticle ($CoFe_2O_4$)
Diameter of the Core	15 nm
Hydrodynamic diameter	50 nm
Fluorescence dye	Rhodamine B
Absorption maxima (λmax)	540 nm
Emission maxima (λem)	625 nm

adjusted at each time point to localize the fluorochromes. Background fluorescence was determined by analyzing unlabeled cells. Image acquisition and analysis was performed using the LSM 5 PASCAL software.

Determination of Intracellular Distribution by Transmission Electron Microscopy (TEM)

MNP@SiO_2(RITC)-PEG-labeled hMSCs were washed with PBS and fixed with 2.5% glutaraldehyde (in pH 7.4 and 0.1 M PBS) for two hours. Subsequently, the glutaraldehyde-fixed specimens were treated with 2% osmium tetroxide buffered in 0.1 mM cacodylate buffer for two hours. The specimens were dehydrated with graded ethanol (50% to 100% ethanol and propylene oxide) (EM Sciences). The samples were embedded in pure Epon resin at 60° C for three days. Next, ultrathin sections were cut with glass knives and a Diatome diamond knife (Reichert-Jung, Vienna, Austria) on an ultramicrotome (RMC MTXL; Tucson, AZ), stained with lead citrate and uranyl acetate (both from EM Sciences), and observed by JEOL-JEM-100 CX Transmission Electron Microscopy (JEOL Ltd. Tokyo, Japan).

In Vitro Cytotoxicity and Cell Proliferation Assay

Cell viability was assessed by a hemocytometer-based trypan blue dye exclusion assay. To exclude the presence of free floating cells in the growth medium, the supernatant of the cells was controlled for floating cells prior to trypsination. The cells were cultured in 96 well plates. The 96 wells were incubated for two hours, four hours, and six hours at different MNP concentrations (0, 0.5, 1, 2, 4 mg/ml). After incubation, the cells were washed three times with PBS and dissociated using trypsin-EDTA. Next, the cells were resuspended with 10 ml of media. A total of 20 μl of the cell suspension was mixed with 30 μl of Trypan blue solution (GIBCO, Gland Island, NY). The fraction of dead cells was determined using a Neubauer's counting chamber.

$$\text{Percent viability} = \frac{\text{Total number of viable cells}}{\text{Total cell count}} \times 100$$

Each value represents the mean ± standard error (SE) of three independent experiments performed in triplicate. The effects of the internalized particles on cell proliferation were studied by comparing the growth curves of MNP@SiO_2(RITC)-PEG-labeled (4 hour incubation time with 4 mg of MNP@SiO_2[RITC]-PEG/ml growth medium) and unlabeled hMSCs. Vision fields were counted under the microscope at 1, 2, 3, and 4 days after labeling. Each value represents the mean ± SE of three independent experiments performed in triplicate.

Magnetic Resonance Imaging

Measurement of T1 and T2 Relaxivity of MNP@SiO_2(RITC)-PEG measured by a 1.5T and 3T MR scanner: MR imaging of the test tubes was performed using a 1.5T and 3T MR scanner (Signa, GE Medical Systems, Milwaukee, WI) and a standard knee coil (Clinical MR Solutions, Brookfield, WI). To avoid susceptibility artifacts from the surrounding air in the scans, all probes were placed in a water-containing plastic container at room temperature (20° C). The concentrations of MNP@SiO_2(RITC)-PEG in each test tube were 0, 10, 30, 50, 100, 200, and 300 μg/ml. To measure the T1 relaxation times, axial spin echo sequences were obtained at multiple TR values of 200, 300, 500, 1,000, 3,000, 5,000, 8,000, 12,000 ms with a fixed TE of 12 ms at 1.5T and 3T. To measure the T2 relaxation times, axial T2-weighted SE images were obtained with a TR of 4,000 ms and increasing TEs of 12, 20, 50, 80, 150, 300, and 500 ms at 1.5T and 3T. All sequences were acquired at a field of view of 130 × 130 mm, a matrix of 256 × 256 pixels, a slice thickness of 5 mm, and one acquisition. The signal intensities of the test tubes, with contrast medium in solution at corresponding iron concentrations, were measured using custom written software for the region of interest analysis. The signal intensity for each pixel, as a function of time, was expressed as follows: $SI = S_o(1-\exp[-TR/T1])$ and $SI = S_o \exp(-TE/T2)$. The T1 relaxivities ($r_1 = \Delta R1$/concentration; $mM^{-1}s^{-1}$) and T2 relaxivities ($r_2 = \Delta R2$/concentration; $mM^{-1}s^{-1}$) at 1.5 and 3T for free solution of MNP@SiO_2(RITC)-PEG were deduced from the linear fit of the $\Delta R1$ and $\Delta R2$ values displayed as a function of the total iron concentration.

MR Phantom Studies and *In Vivo* MR imaging: For MR phantom imaging, hMSCs were cultured in MSCBM containing MNP of various concentrations (MNP concentrations of 0.5, 1, 2 and 4 mg/ml). After incubation, cells were washed three times with PBS, trypsinized, and collected in 50 ml tubes. Next, the samples were prepared by suspending 10^5 and 5×10^5 cells in 350 μl 4% gelatin (Wako Pure Chemical Industries, Osaka, Japan). The cell suspensions were loaded onto 96 well plates and allowed to solidify at 4 ℃. The experimental MR imaging of a phantom of labeled hMSCs was performed with a 3T MR scanner (Signa, GE Healthcare, Milwaukee, WI) using the three-dimensional b-SSFP (balanced Steady-State Free Precession) pulse sequence (FIESTA; Fast Imaging Employing Steady State Acquisition, GE Healthcare, Milwaukee, WI) with a TR of 8.8 ms, TE of 4.1 ms, field of view of 100 × 100 mm, and a voxel size of 1 × 1 × 1 mm^2. The region of interest for signal

intensity (SI) measurement was 20 mm^2. The percent change of SI was calculated using the following equation: $\Delta SI = (SI_{labeled} - SI_{unlabeled})/ SI_{unlabeled} \times 100\%$, where $SI_{labeled}$ and $SI_{unlabeled}$ were the SI of the labeled and unlabeled cells, respectively. For animal experiments, hMSCs were cultured in MSCBM containing 4 mg of MNP@SiO_2(RITC)-PEG/ml media for four hours. After incubation and washing, the 0.5–1 $\times 10^6$ labeled cells/200μl were injected into a kidney of SD (Sprague Dauley) rats and different numbers of MNP@SiO_2(RITC)-PEG-labeled hMSCs (1×10^4, 1×10^5, 0.5×10^6, 1×10^6 mg/ml) were injected subcutaneously into nude mice. Six hours after injection of the labeled hMSCs, sequential MR imaging of SD rats and nude mice were obtained with a 3T MR scanner. Three pulse sequences were applied in the axial and coronal plane: 3D FIESTA (TR/TE/flip angle: 8.4/4.1/35), FSE (fast spin echo, TR/TE/flip angle: 3,500/89.8/90), and MGRE (multiple gradient-recalled echo, TR/TE/flip angle: 800/13.4/20).

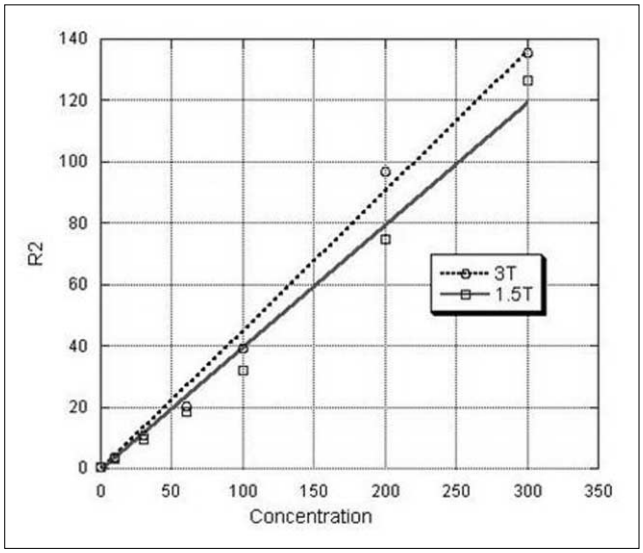

Fig. 1. Transverse relaxation rate (R2) versus MNP@SiO_2(RITC)-PEG concentration at 1.5T and 3T.

In Vivo and Ex Vivo Fluorescence Imaging

For optical imaging, nude mice were injected subcutaneously with the different numbers of MNP@SiO_2(RITC)-PEG-labeled hMSCs (1×10^4, 1×10^5, 0.5×10^6, 1×10^6 mg/ml) and 1×10^5 unlabeled hMSCs for the controls. We performed *in vivo* fluorescence imaging using a Kodak Image Station 4000 mm digital imaging system. And also we excised the kidney with labeled hMSCs of SD rats after performing MRI and subsequently performed *ex vivo* fluorescence imaging to confirm the presence of the fluorescence signal coming from the transplanted labeled

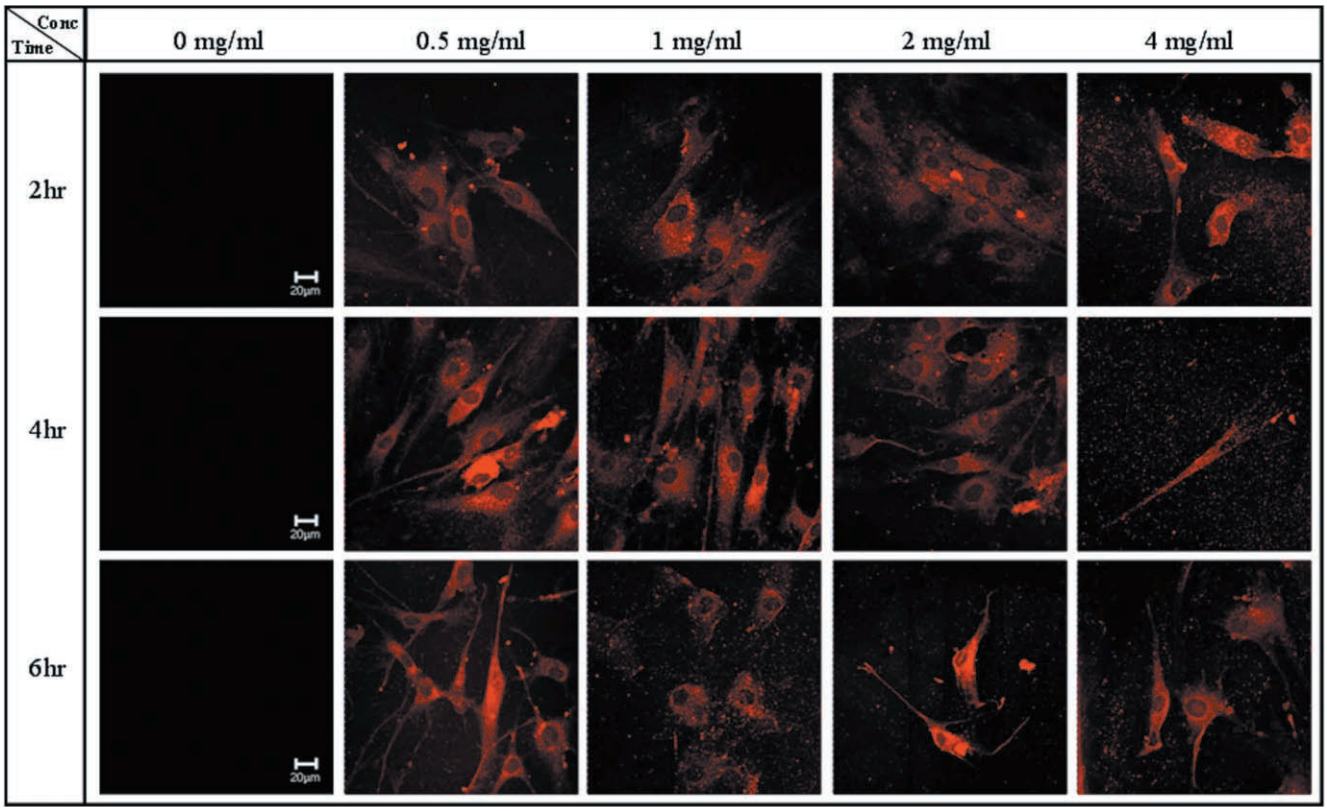

Fig. 2. Cellular distribution of MNP@SiO_2(RITC)-PEG in human mesenchymal stem cells. Confocal fluorescence images of human mesenchymal stem cells cultured with different concentrations of MNP@SiO_2(RITC)-PEG (0, 0.5, 1, 2 and 4 mg/ml) for 2, 4, and 6 hours.

hMSCs.

RESULTS

MNP@SiO_2(RITC)-PEG showed both superparamagnetic and fluorescent properties. The r_1 and r_2 relaxivity values of the MNP@SiO_2(RITC)-PEG were 0.33 and 398 mM^{-1} s^{-1} at 1.5T, respectively, and 0.29 and 453 mM^{-1} s^{-1} at 3T, respectively (Fig. 1). The effective internalization of MNP@SiO_2(RITC)-PEG into the hMSCs was observed by confocal laser scanning fluorescence microscopy as shown in Figure 2. In these fluorescence images, the hMSCs cultured with MNP@SiO_2(RITC)-PEG took up a substantial amount of MNP@SiO_2(RITC)-PEG as clearly identified by intracellular fluorescence signals, whereas those cultured without MNP@SiO_2(RITC)-PEG were not detected by confocal LSM. There are no differences in the rate of uptake with increasing incubation concentrations of

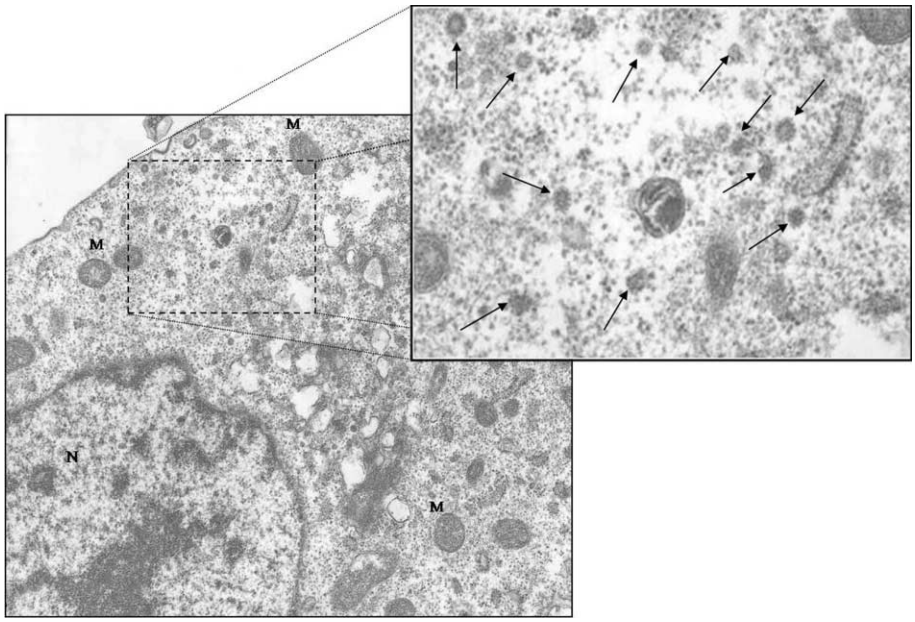

Fig. 3. Transmission electron microscopy images of human mesenchymal stem cells embedded in MNP@SiO_2(RITC)-PEG. Human mesenchymal stem cells were treated with 4 mg of MNP@SiO_2 (RITC)-PEG/ml medium for four hours, which was then processed for transmission electron microscopy study. MNP@SiO_2 (RITC)-PEG (arrows) exhibited after internalization into cells. MNP@SiO_2 (RITC)-PEG-treated cell (× 10,000, 20,000). N = nucleus, M = mitochondria

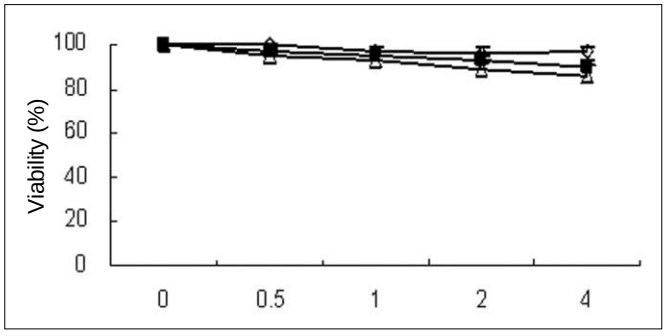

A

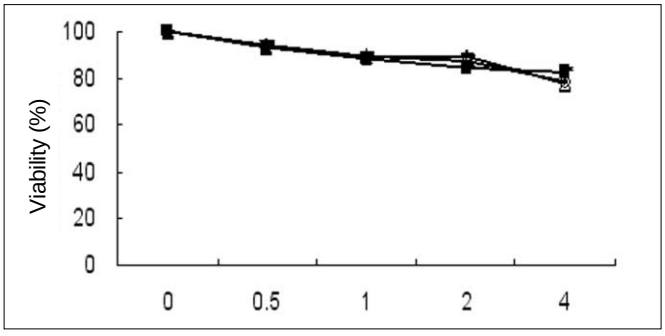

B

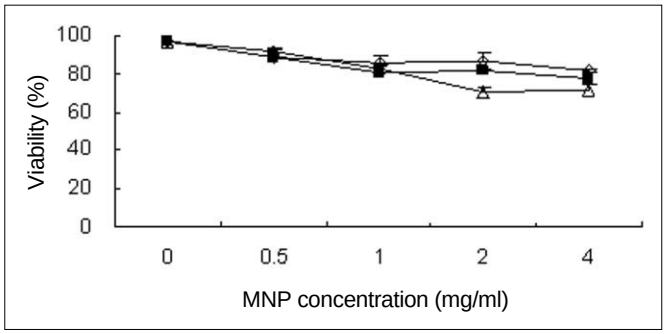

C

Fig. 4. Cell viability. Human mesenchymal stem cells were incubated for 2 (◇), 4, (■) and 6 hours (△) with different magnetic nanoparticle concentrations (0, 0.5, 1, 2, 4 mg/ml) after 0 (**A**), 2 (**B**), and 4 days (**C**).

MNP@SiO_2(RITC)-PEG. Confocal LSM showed that MNP@SiO_2(RITC)-PEG particles resided in the cytoplasm and outside of the nucleus of a cell. These results confirmed that the MNP@SiO_2(RITC)-PEG particles exhibited a strong role in targeting hMSCs and that the cellular uptake of MNP@SiO_2(RITC)-PEG particles can be visualized by fluorescence imaging at the cellular level. We examined the localization and morphology of MNP@SiO_2(RITC)-PEG particles by electron microscopy. The characteristic granular morphology of these MNP@SiO_2(RITC)-PEG particles was identified only in MNP@SiO_2(RITC)-PEG -labeled hMSCs and never in unlabeled controls. The TEM images showed that MNP@SiO_2(RITC)-PEG were indeed internalized into the cells and mainly resided in the cytoplasm (Fig. 3).

A trypan blue exclusion assay showed that there was no increase in the number of floating cells in the supernatant as determined by visual control under the microscope. In addition, the number of adherent cell was not significantly different between the controls and the labeled cells (Fig. 4). After incubating for two hours with 0.5 mg MNP@SiO_2(RITC)-PEG/ml growth medium, we observed no significant difference in the viability between controls (unlabeled cells) and MNP@SiO_2(RITC)-PEG-labeled cells. After incubating for two hours at different concentrations of MNP@SiO_2(RITC)-PEG, the percentage of viable cells was greater than 96%. After incubating for four hours at different concentrations of MNP@SiO_2(RITC)-PEG, cell viability decreased by 3.5% (0.5 mg/ml), 4.9% (1 mg/ml), 7.2% (2 mg/ml), and 9.8% (4 mg/ml). After incubating for six hours at different concentrations of MNP@SiO_2(RITC)-PEG, cell viability decreased by 5.4% (0.5 mg/ml), 6.9% (1 mg/ml), 10.9% (2 mg/ml), and 14.4% (4 mg/ml). The proliferation of MNP@SiO_2(RITC)-PEG-labeled cells did not significantly differ from the controls (Fig. 5). Moreover, the mean doubling time for the labeled and unlabeled cells was 26.8 hours.

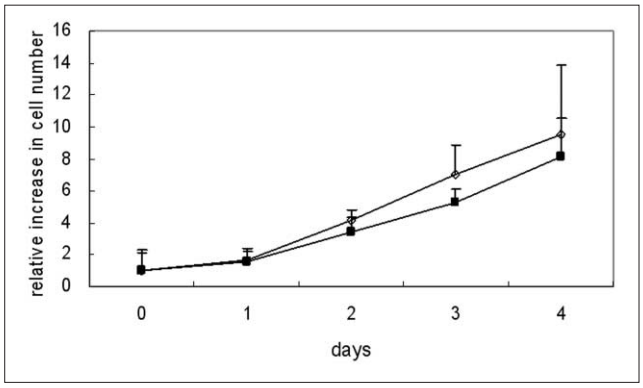

Fig. 5. Proliferation index of human mesenchymal stem cells, which were incubated for four hours with 4 mg/ml MNP@SiO_2(RITC)-PEG is shown (■). Control (◇).

The MR images using the FIESTA sequence from the *in vitro* gelatin phantom of 5×10^5 labeled and unlabeled MSCs of 2, 4, 6-hour culture, 1×10^5 labeled and unlabeled MSCs of 2, 4, 6-hour culture were shown in Figure 6. The SI changes of the labeled cells from the 4-hour culture were −20%, −36%, −67%, and −80% at each incubation concentration of MNP@SiO_2(RITC)-PEG (0.5, 1.0, 2.0, and 4.0 mg/ml, respectively). The SI decrease for the 5×10^5 labeled cells at the 4 mg/ml incubation concentration was 71%, 80%, and 80% at 2, 4, and 6-hours of incubation, respectively. The SI decrease of 1×105 labeled cells at the 4 mg/ml incubation concentration was 39%, 77%, and 60% at 2, 4, and 6-hours of incubation, respectively. The overall SI change for the *in vitro* gelatin plate MR phantom of the labeled hMSCs was maximal at the four hour incubation time and 4 mg/ml incubation concentration of

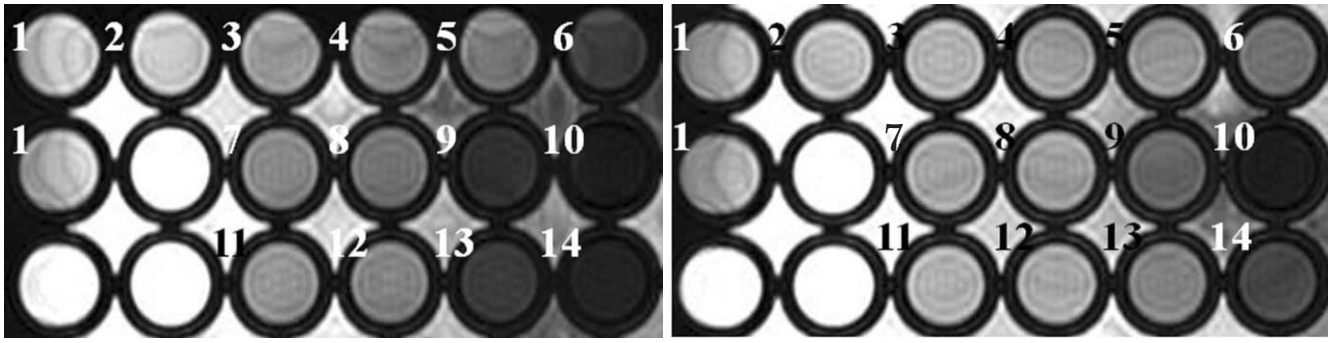

Fig. 6. Experimental MRI of phantom of labeled human mesenchymal stem cells placed in 4% phantom gelatin in plastic wells. Coronal FIESTA (GE, b-SSFP) sequence image of phantom shows marked decrease in signal intensity with increasing magnetic nanoparticle concentration.
A. 5×10^5 cells in 4% gelatin, **B.** 1×10^5 cells in 4% gelatin.
1 = gelatin, 2 = unlabeled hMSCs in 4% gelatin, 3–6 = labeled hMSCs with 2-hour incubation; 7–10 = 4-hour incubation, 11–14 = 6-hour incubation. 3, 7, 11 = labeled human mesenchymal stem cells at magnetic nanoparticle concentration of 0.5 mg/ml, 4, 8, 12, at 1 mg/ml; 5, 9, 13, at 2 mg/ml; 6, 10 ,14, at 4 mg/ml.

MNP@SiO_2(RITC)-PEG. The labeled hMSCs containing tubes revealed a color fluorescent signal in the tubes. In order to examine the ability of MRI to detect transplanted stem cells, we injected labeled hMSCs into the kidneys of SD rats. The animals were imaged *in vivo* at six hours after implantation of the labeled cells with several pulse sequences. The imaging revealed a significant drop in signal intensity at the area of cell implantation (Fig. 7). However, the fluorescence signal cannot be detected in the rats *in vivo*. The fluorescent signal coming from the transplanted labeled hMSCs was detected at the excised kidney. The fluorescence signal of the MNP@SiO_2(RITC)-PEG-labeled hMSCs could be imaged *in vivo* with a subcutaneous injection of a variable number of the labeled hMSCs into nude mice (Fig. 8). The subcutaneously inoculated labeled hMSCs showed a fluorescent signal in nude mice. However, no fluorescent signal was observed when the labeled cells were deeply seated in the body of the mice. The depth of the subcutaneous injection and imaged sites or positions significantly influenced the detectability of the fluorescent signal coming from the injected labeled MSCs.

DISCUSSION

Superparamagnetic iron oxide nanoparticles and their composites are the most popular contrast agents for tracking and studying stem cells by MRI. Unfortunately, the internalizing efficiency of the iron oxide nanoparticles is generally low. The labeling of the cultured stem cells with superparamagnetic iron oxide nanoparticles requires long-term incubation; from approximately 10 hours to a few days in previous studies, despite the various coating material substitutes (14, 15, 21). Popular MRI contrast agents, such as Feridex (AMAG Pharmaceuticals Inc., Cambridge, MA), require the addition of a transfecting agent (internalization agent) for efficient cellular uptake (22). In this study, we demonstrated that the synthesized MNP@SiO_2(RITC)-PEG could be efficiently internalized into hMSCs without the assistance of the transfecting agent. In addition, the incubation time used to label the hMSCs was short and the nanoparticles were substantially

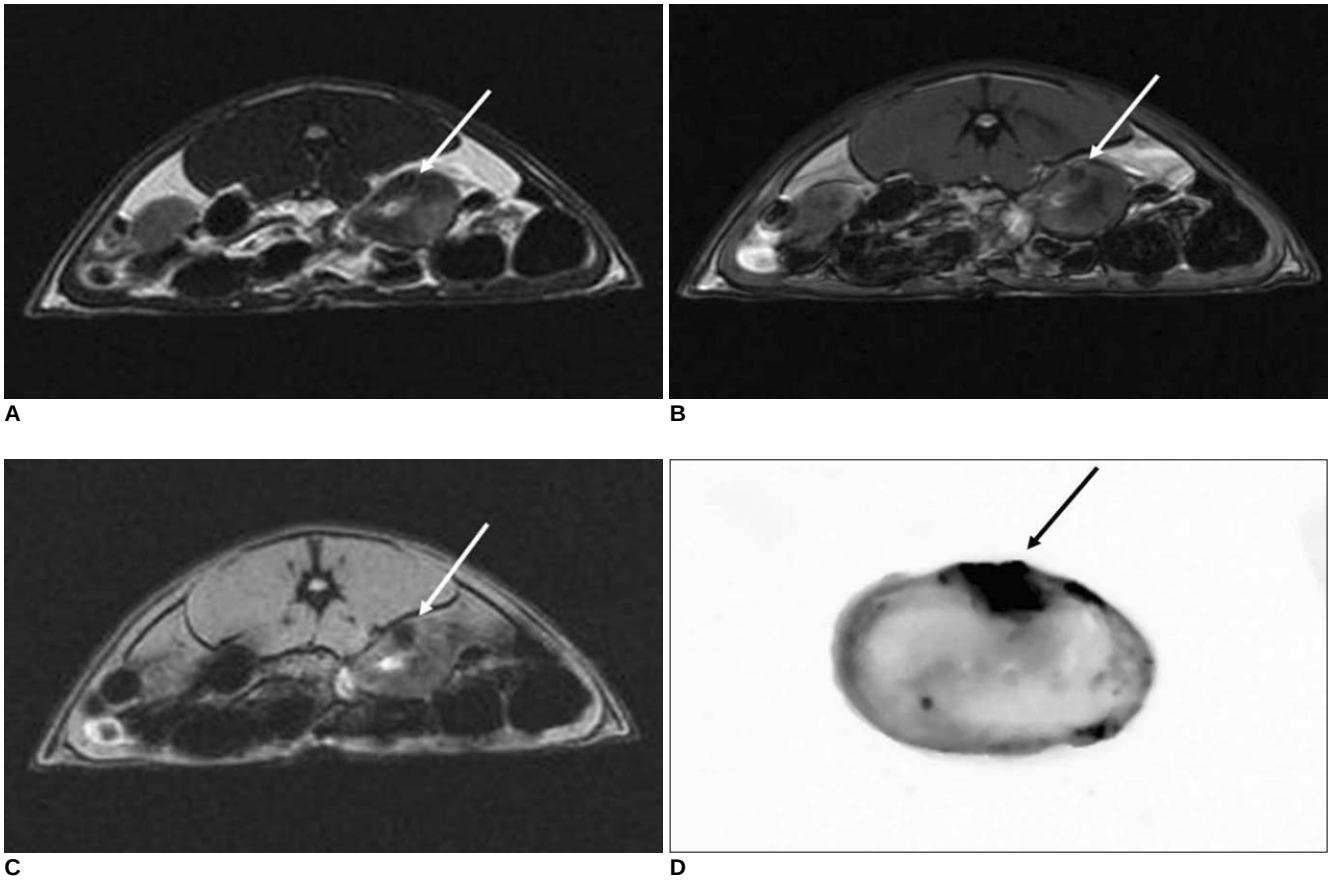

Fig. 7. Sequential *in vivo* MR imaging (3T, 3.0 mm slices) and fluorescence imaging of SD rat after injection with MNP@SiO_2(RITC)-PEG-labeled human mesenchymal stem cells.
A-D. MR images with fast spin echo (TR/TE: 3,500/89.8) (**A**), 3D fast imaging employing steady state acquisition (TR/TE/flip angle: 8.4/4.1/35) (**B**), multiple gradient-recalled echo (TR/TE/flip angle: 800/13.4/20) (**C**), and fluorescent signal coming from labeled human mesenchymal stem cells in kidney of SD rat (arrows) can only be detected in excised state (**D**).

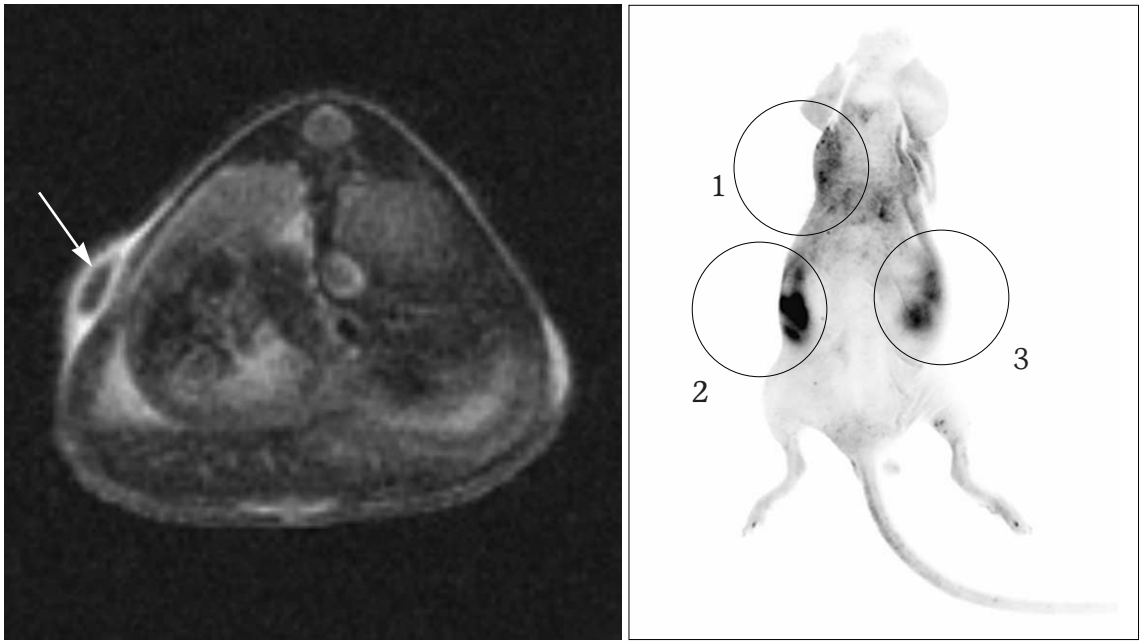

Fig. 8. *In vivo* MR imaging (**A**) and fluorescence imaging (**B**) of nude mouse after subcutaneous injection of labeled and unlabeled human mesenchymal stem cells with MNP@SiO_2(RITC)-PEG (1 = 1×10^5 unlabeled human mesenchymal stem cells for control, 2 = 1×10^6 labeled human mesenchymal stem cells, 3 = 1×10^5 labeled human mesenchymal stem cells). Labeled human mesenchymal stem cells are clearly seen as dark dot (arrow) in subcutaneous layer of nude mouse on axial scan of fast spin echo sequence. Fluorescent signal of subcutaneously injected human mesenchymal stem cells is detected at injection sites of labeled cells. Injection sites of unlabeled cells shows autofluorescence-induced artifact.

internalized during the first two hours of incubation. The maximal signal drop in MRI was seen at the four hour incubation time amongst the comparison of the 2, 4 and 6 hours incubation times. The improved labeling efficiency with the short incubation time and the independent transfecting agent might be contributed by the surface modification with PEG groups. PEG coatings of silica shells provides biocompatibility by preventing nanoparticle agglomeration and nonspecific adsorption of proteins to the nanoparticles, thus increasing the particle blood circulation time and the efficiency of their internalization by targeted cells when introduced *in vivo* (23). A recent study revealed that amorphous silica may present toxicity concerns at high doses (24). The cytotoxic effects of silica nanoparticles can be significantly reduced by surface modification of silica shells with chitosan or PEG (20, 24).

The surface properties of nanoparticles influence its uptake mechanisms. Further, there are different mechanisms for the cellular internalization of the magnetic nanoparticles. However, the best known is the clathrin-dependent endocytosis (25, 26). Kim et al. (26) showed that the uptake of magnetic nanoparticles into the cells is an energy-dependent process and it is mediated through endosomes. After entering the cytoplasm, the ingested nanoparticles are delivered to early endosomes and then transported to the lysosome. The ingested nanoparticles can be stored in different compartments (such as mitochondria) in the cytoplasm (25). The TEM images in this study showed the intracytoplasmic localization of the internalized nanoparticles with a granular appearance. The effective energy-dependent endocytic uptake of the nanoparticles may allow the simultaneous intracellular uptake of the drugs- or genes-of-interest by the formation of complex molecules when the surface of the nanoparticles is optimally modified (26).

We demonstrated that MNP@SiO_2(RITC)-PEG was less toxic without affecting the cell viability and cell proliferation of hMSCs after MNP@SiO_2(RITC)-PEG-treated cells were incubated with growth medium for various lengths of time. These facts indicated that MNP@SiO_2(RITC)-PEGs are quite biocompatible. The noncovalent surface modification of the nanoparticles has a serious limitation for biological applications, because the exposed metal ion on the surface of nanoparticles can cause metal elemental toxicities in cells (*in vivo* model) (27). In our research, silica (SiO_2) was selected for the surface modification of MNPs because it is a good biocompatible material and resistant to decomposition *in vivo* (20). Consequently, silica-coated core-shell nanoparticles have been extensively studied over the past decade (25), and were recently synthesized with a functionalized surface for bioconjugation through various simple methods that are

applicable in biological systems. To improve the versatility of silica-coated core-shell nanomaterials, an organic fluorescent dye was incorporated into the silica shell. Thus, the magnetic and fluorescence properties enable the dual detection of the silica-coated core-shell magnetic nanoparticles (MNP@SiO_2). The additional advantage provided by the incorporation of a fluorescent dye into the silica shell is the significant increase in photochemical stability, resulting in minimal photobleaching even after multiple exposures. This aforementioned topic is of great importance among researchers using confocal laser scanning microscopy (20).

Several imaging modalities are currently in use for the molecular and cellular imaging techniques. Unlike the previous approaches in stem cell research that required the processing of fixed tissue samples, these imaging modalities enable the imaging of living, intact transplanted cells *in vivo*. Since each imaging modality has its own merits and disadvantages, multi-modality imaging has emerged as a strategy that combines the strengths of different imaging methods. Multi-modality imaging can be achieved by the development of true hybrid systems that collect images under the same condition and by the development of sophisticated technologies for image registration and fusion. The development of multifunctional contrast agents can be another way to develop multimodal imaging. Recently, the synthesis of similar nanoparticles for dual modal imaging was reported by various authors (18, 23, 28, 29). They reported that the bifunctional nanoparticles can be used for magnetic resonance as well as the optical imaging of human stem cells, brain tumor, and sentinel lymph node. Despite the rapid advances in optical imaging, there are several challenges in the development of highly sensitive and photostable nanoparticles with a substantial penetration depth. We used organic dyes (RITC) to provide the magnetic nanoparticles with their fluorescent property. The use of organic dyes for stem cell imaging might be limited, since these dyes are often cleared rapidly and thus require a large quantity of dye for optical imaging. For this reason, the light in the near-infrared region of 650 nm–900 nm is most commonly used in practical applications (30). It is still necessary to develop suitable optical probes for deep tissue optical imaging.

The quality of a contrast agent for MRI is dependent on its relaxivity. In this study, the synthesized nanoparticles in an aqueous solution showed significantly higher r_2 relaxivity (398 mM^{-1} s^{-1} at 1.5T and 453 mM^{-1} s^{-1} at 3T) and a higher r_2/r_1 relaxivity ratio compared to commercially available superparamagnetic iron oxide nanoparticles (ferumoxide and ferucarbotran). Thus, the T2 effect dominates and the MNP@SiO_2(RITC)-PEG can be a good T2/T2* agent. The contrast agents exhibit magnetic and optical properties. This bifunctional property enables the simultaneous detection by MRI and optical imaging. We found that MRI and fluorescence imaging can facilitate the identification of labeled stem cells, both *in vitro* and *in vivo* and thus, provide an accurate estimate of cell delivery. However, fluorescence imaging showed limitations in penetration depth and consequently visualized the subcutaneously injected labeled hMSCs. However, the deep seated stem cells in small animal cannot be visualized. Although the biomedical application of optical imaging is still limited, the combination of MRI and optical imaging can extend their utilities for molecular and cellular imaging.

In the past decade, the therapeutic use of mesenchymal stem cells in tissue regeneration has been under intense investigation. To date, the true functional role of MSCs *in vivo* is not clear (31). MSCs may act by paracrine or even endocrine mechanisms related to the production of a broad array of mediators and growth factors with immunosuppressive, anti-inflammatory, antiapoptotic and proliferative effects (32). There is a general consensus that the field of MSC biology is significantly less developed than other stem cell fields. Therefore tracking the distribution and migration of the transplanted MSCs in the patients are important for the development of their therapeutic use. One innovative development for stem cell tracking is the multimodal imaging which might be a powerful method for *in vivo* visualization of transplanted stem cells by using the combined strengths of each modality. In this study, we demonstrated a bifunctional (magneto/optical) contrast agent using a synergistic integration of magnetic nanoparticles with fluorescent molecules to serve as a good imaging probe for stem cell research. Owing to its bifunctional property, dual modality detection was simultaneously achieved using a single material. The dual modal imaging using magneto/optical nanoparticles is expected to give good anatomical information via MRI, along with more detailed subcellular information via fluorescence imaging taken at the same point.

In this study, we have demonstrated that MNP@SiO_2(RITC)-PEG could be efficiently internalized into hMSCs and was less toxic (no significant effect on cell viability and proliferation). As well, the hMSCs labeled with MNP@SiO_2(RITC)-PEG were detected *in vitro* and *in vivo*, and noninvasively traced by both optical imaging and MRI. In conclusion, although further investigations are needed for stem cell tracking, this study suggests MNP@SiO_2(RITC)-PEG is a useful contrast agent for stem cell imaging, which is suitable for a bimodal detection by MRI and optical imaging.

Acknowledgement

This study was supported by a grant from the Seoul Research & Business Development Program 10548 and by the Interdisciplinary Research Initiatives Program set forth by the College of Natural Sciences and the College of Medicine, Seoul National University (2007).

References

1. Bussolati B, Camussi G. Adult stem cells and renal repair. *J Nephrol* 2006;19:706-709
2. Strauer BE, Kornowski R. Stem cell therapy in perspective. *Circulation* 2003;107:929-934
3. Daldrup-Link HE, Rudelius M, Piontek G, Metz S, Brauer R, Debus G, et al. Migration of iron oxide-labeled human hematopoietic progenitor cells in a mouse model: in vivo monitoring with 1.5-T MR imaging equipment. *Radiology* 2005;234:197-205
4. Frangioni JV, Hajjar RJ. In vivo tracking of stem cells for clinical trials in cardiovascular disease. *Circulation* 2004;110:3378-3383
5. Hoshino K, Ly HQ, Frangioni JV, Hajjar RJ. In vivo tracking in cardiac stem cell-based therapy. *Prog Cardiovasc Dis* 2007;49:414-420
6. Suzuki Y, Yeung AC, Yang PC. Cardiovascular MRI for stem cell therapy. *Curr Cardiol Rep* 2007;9:45-50
7. Chang NK, Jeong YY, Park JS, Jeong HS, Jang S, Jang MJ, et al. Tracking of neural stem cells in rats with intracerebral hemorrhage by the use of 3T MRI. *Korean J Radiol* 2008;9:196-204
8. Weissleder R, Cheng HC, Bogdanova A, Bogdanov A Jr. Magnetically labeled cells can be detected by MR imaging. *J Magn Reson Imaging* 1997;7:258-263
9. Yeh TC, Zhang W, Ildstad ST, Ho C. Intracellular labeling of T-cells with superparamagnetic contrast agents. *Magn Reson Med* 1993;30:617-625
10. Moore A, Basilion JP, Chiocca EA, Weissleder R. Measuring transferrin receptor gene expression by NMR imaging. *Biochim Biophys Acta* 1998;1402:239-249
11. Handgretinger R, Lang P, Schumm M, Taylor G, Neu S, Koscielank E, et al. Isolation and transplantation of autologous peripheral CD34+ progenitor cells highly purified by magnetic-activated cell sorting. *Bone Marrow Transplant* 1998;21:987-993
12. Bulte JW, Douglas T, Witwer B, Zhang SC, Strable E, Lewis BK, et al. Magnetodendrimers allow endosomal magnetic labeling and in vivo tracking of stem cells. *Nat Biotechnol* 2001;19:1141-1147
13. Jendelová P, Herynek V, DeCroos J, Glogarova K, Andersson B, Hájek M, et al. Imaging the fate of implanted bone marrow stromal cells labeled with superparamagnetic nanoparticles. *Magn Reson Med* 2003;50:767-776
14. Song M, Moon WK, Kim Y, Lim D, Song IC, Yoon BW. Labeling efficacy of superparamagnetic iron oxide nanoparticles to human neural stem cells: comparison of ferumoxides, monocrystalline iron oxide, cross-linked iron oxide (CLIO)-NH2 and tat-CLIO. *Korean J Radiol* 2007;8:365-371
15. Hill JM, Dick AJ, Raman VK, Thompson RB, Yu ZX, Hinds KA, et al. Serial cardiac magnetic resonance imaging of injected mesenchymal stem cells. *Circulation* 2003;108:1009-1014
16. Huh YM, Jun YW, Song HT, Kim S, Choi JS, Lee JH, et al. In vivo magnetic resonance detection of cancer by using multifunctional magnetic nanocrystals. *J Am Chem Soc* 2005;127:12387-12391
17. Mulder WJ, Koole R, Brandwijk RJ, Storm G, Chin PT, Strijkers GJ, et al. Quantum dots with a paramagnetic coating as a bimodal molecular imaging probe. *Nano Lett* 2006;6:1-6
18. Lu CW, Hung Y, Hsiao JK, Yao M, Chung TH, Lin YS, et al. Bifunctional magnetic silica nanoparticles for highly efficient human stem cell labeling. *Nano Lett* 2007;7:149-154
19. Yoon TJ, Kim JS, Kim BG, Yu KN, Cho MH, Lee JK. Multifunctional nanoparticles possessing a "magnetic motor effect" for drug or gene delivery. *Angew Chem Int Ed Engl* 2005;44:1068-1071
20. Yoon TJ, Yu KN, Kim E, Kim JS, Kim BG, Yun SH, et al. Specific targeting, cell sorting, and bioimaging with smart magnetic silica core-shell nanomaterials. *Small* 2006;2:209-215
21. Jendelová P, Herynek V, Urdziková L, Glogarová K, Kroupová J, Andersson B, et al. Magnetic resonance tracking of transplanted bone marrow and embryonic stem cells labeled by iron oxide nanoparticles in rat brain and spinal cord. *J Neurosci Res* 2004;76:232-243
22. Frank JA, Miller BR, Arbab AS, Zywicke HA, Jordan EK, Lewis BK, et al. Clinically applicable labeling of mammalian and stem cells by combining superparamagnetic iron oxides and transfection agents. *Radiology* 2003;228:480-487
23. Veiseh O, Sun C, Gunn J, Kohler N, Gabikian P, Lee D, et al. Optical and MRI multifunctional nanoprobe for targeting gliomas. *Nano Lett* 2005;5:1003-1008
24. Chang JS, Chang KL, Hwang DF, Kong ZL. In vitro cytotoxicitiy of silica nanoparticles at high concentrations strongly depends on the metabolic activity type of the cell line. *Environ Sci Technol* 2007;41:2064-2068
25. Huang DM, Hung Y, Ko B, Hsu SC, Chen WH, Chien CL, et al. Highly efficient cellular labeling of mesoporous nanoparticles in human mesenchymal stem cells: implication for stem cell tracking. *FASEB J* 2005;19:2014-2016
26. Kim JS, Yoon TJ, Yu KN, Noh MS, Woo M, Kim BG, et al. Cellular uptake of magnetic nanoparticle is mediated through energy-dependent endocytosis in A549 cells. *J Vet Sci* 2006;7:321-326
27. Kirchner C, Liedl T, Kudera S, Pellegrino T, Muñoz Javier A, Gaub HE, et al. Cytotoxicity of colloidal CdSe and CdSe/ZnS nanoparticles. *Nano Lett* 2005;5:331-338
28. Kircher MF, Mahmood U, King RS, Weissleder R, Josephson L. A multimodal nanoparticle for preoperative magnetic resonance imaging and intraoperative optical brain tumor delineation. *Cancer Res* 2003;63:8122-8125
29. Kim JS, Yoon TJ, Kim HK, Kim SS, Chae HS, Choi MG, et al. Sentinel lymph node mapping of the stomach using fluorescent magnetic nanoparticles in rabbits. *Korean J Gastroenterol* 2008;51:19-24
30. Weissleder R. A clearer vision for in vivo imaging. *Nat Biotechnol* 2001;19:316-317
31. Summer R, Fine A. Mesenchymal progenitor cell research: limitations and recommendations. *Proc Am Thorac Soc* 2008;5:707-710
32. Bussolati B, Tetta C, Camussi G. Contribution of stem cells to kidney repair. *Am J Nephrol* 2008;28:813-822